

Short Communication

Effect of Silicon Addition on Electrochemical Corrosion Resistance of Carbon Steel in Concrete Pore Solution

Shufang Li^{1,*}, Jian Zhang²

¹ School of Civil Engineering, Chongqing Vocational Institute of Engineering, Chongqing 402260, China

² CMCU Engineering Co., Ltd, Chongqing 400039, China

*E-mail: lsf2008zj@163.com

Received: 23 August 2020 / Accepted: 9 October 2020 / Published: 31 October 2020

The effects of Si content on the corrosion behavior and passivation of carbon steel bars in concrete pore solution were studied analytically, and its enhanced corrosion resistance was considered. Electrochemical impedance spectroscopy analysis and polarization techniques were used to investigate the electrochemical corrosion behavior of the samples. The lower mass-loss rate for the steel bar with 0.57 wt% Si content in the initial corrosion indicated an improvement of the corrosion resistance in the carbon steel matrix before the creation of a dense rust layer on the sample surface. The polarization plots exhibited that the steel bar with 0.57% Si content had minimum corrosion-current density compared to the other specimens which were in passive state during the experiment. The electrochemical results show that micro-alloying of Si element in the carbon steel bar matrix improved its corrosion resistance against chloride ion attack and delayed the corrosion initiation into the steel matrix. FESEM images of the specimens indicated that the surface of the carbon steel bar with 0.57% Si was smooth and no noticeable corrosion was found.

Keywords: Silicon alloying; Carbon steel; Electrochemical corrosion; Concrete pore solution

1. INTRODUCTION

Carbon steels and its alloys are extensively used in numerous industries such as aerospace, automotive and construction due to the excellent formability and high production rate [1]. Aggressive solutions such as saline environments are the most corrosive in nature for carbon steel alloys than the other corrosive environment [2, 3]. Hence, it is desirable to consider the protection of corrosion steels in saline solutions [4, 5]. The corrosion resistance of carbon steel depends on the stability and the presence of oxide film on its surface. Researchers have done a lot of research to develop the durability of the concrete structures [6, 7]. Recently, there are many approaches to extend lifespan of the

reinforced structures immersed to the corrosive environments, containing the coated materials on steel reinforcement, corrosion inhibitors and micro-alloyed steel reinforcement [8-10].

By addition of anti-corrosion alloy elements, such as copper, chromium, aluminum, nickel, molybdenum and silicon, the corrosion behavior of carbon steel rebar may be enhanced in comparison to the common carbon steel bars [11-13]. However, because of the use of the alloy element in small quantities, the production cost can be remarkably reduced. Thus, these alloyed rebars have great potential which can be utilized as an alternative to the carbon steel rebars with a long operating life in a corrosive environment [14-16]. Furthermore, alloying elements are added into the carbon steel to enhance its mechanical properties such as crash worthiness, formability, elongation, strain strength and elasticity limit. Silicon is present in high-strength alloy steels to improve their corrosion resistance and mechanical.

However, many studies have been done to evaluate the alloying effect on corrosion behavior of carbon steel rebars, the effect of silicon alloying on electrochemical corrosion resistance of carbon steel rebars has never been investigated in concrete pore solution. Therefore, this study aimed to evaluate the efficiency of Si micro-alloying addition in carbon steel on corrosion resistance using electrochemical characterizations.

2. MATERIALS AND METHOD

Carbon steel bars with a diameter of 25 mm were purchased from the open market in Chongqing, China and analyzed with the Phenom proX scanning electron microscope at the Materials Characterization Laboratory. Table 1 shows the chemical composition of carbon steel bars used in this study.

Table 1. The chemical composition of carbon steel bars with different Si content (wt%)

Steels	C	Si	Mn	S	P	Nb	Fe
C1	0.32	0.42	1.63	0.024	0.02	0.055	Residual
C2	0.32	0.47	1.63	0.024	0.02	0.055	Residual
C3	0.32	0.52	1.63	0.024	0.02	0.055	Residual
C4	0.32	0.57	1.63	0.024	0.02	0.055	Residual

The corrosion and passivation behaviors of carbon steel bars in the concrete pore solution with Cl ions were analytically considered by electrochemical corrosion assessments. A saturated aqueous solution of Ca(OH)₂ with pH value of 13 was selected as the simulated concrete pore solution. Electrochemical corrosion assessments were performed in saturated Ca(OH)₂ solution containing 3.5% NaCl through an advanced potentiostat by a traditional three-electrode method which contained a saturated calomel and a Pt wire as reference and counter electrodes, respectively. Furthermore, all carbon steel bars as working electrodes were polished, cleaned through acetone and dried by warm air. A minimum three replicates were carried out for each specimen. Electrochemical impedance spectroscopy (EIS, Wuhan CorrTest Instruments Corp., Ltd.) were done at 10 mV amplitude with a scanning range of 0.1 MHz and 0.01 Hz after one month immersion time. EIS experiments were

performed with a model EA-201 Electro Analyzer (chemilink systems), equipped with a personal computer that was used for electrochemical measurement and treating of data. The potentiodynamic polarization (CorrTest Instruments Corp., Ltd., China) measurement was conducted from 0.3V at 1 mV/s scanning rate after one month immersion time. The scanning electron microscope (SEM) was used to consider the surface morphologies of the samples.

3. RESULTS AND DISCUSSION

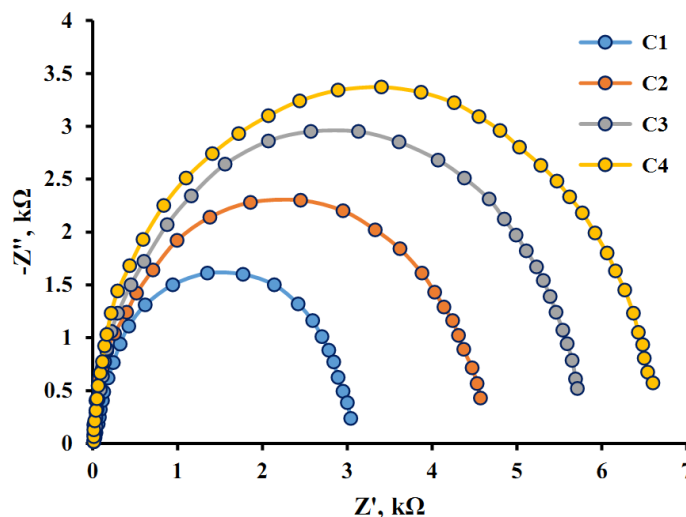


Figure 1. EIS plots of the carbon steel bars with different content of Si in concrete pore solution at pH value of 13 with a scanning range of 0.1 MHz and 0.01 Hz after one month immersion time.

In order to study the effect of Si micro-alloyed steel on the corrosion resistance of bars in concrete pore solution containing 3.5% NaCl, the EIS analysis was conducted. Figure 1 shows the Nyquist plots from EIS measurement. The increase in Si concentration leads to an enhancement in the capacitive loop radius which reveals improvement of the corrosion resistance in the carbon steel bar. Figure 2 shows a used equivalent circuit for modeling the impedance spectra. R_s presents the solution resistance. R_{ct} and R_f are the resistance of the charge-transfer resistance and passive film, respectively [17]. C_{dl} and C_f are the double-layer and passive film/solution interface capacitances, respectively [18, 19].

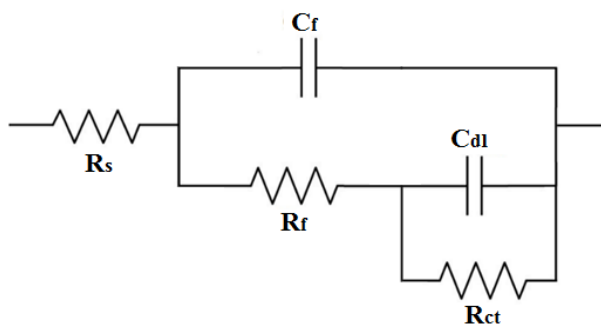


Figure 2. A used equivalent circuit for modeling the impedance spectra

Polarization resistance (R_p) is an assessable indicator to describe the corrosion behavior of carbon steel bars in concrete pore solution. The higher value of R_p presents the superior corrosion resistance.

Table 2. Electrochemical parameters derived from the EIS results

Steels	R_s ($\Omega \text{ cm}^2$)	R_f ($\text{k}\Omega \text{ cm}^2$)	C_f ($\mu\text{F cm}^{-2}$)	R_{ct} ($\text{k}\Omega \text{ cm}^2$)	C_{dl} ($\mu\text{F cm}^{-2}$)
C1	37.1	0.178	4.6	3.08	6.6
C2	34.3	0.346	3.3	4.76	4.9
C3	31.5	0.412	2.7	5.91	3.5
C4	34.7	0.583	2.1	6.83	2.6

As shown in table 2, increasing the Si content in steel bars reveals a considerable increase in R_p value showing a higher corrosion resistance in C4 sample with 0.57% Si.

C_f is associated to the passive layer thickness as revealed in the following equation [20]:

$$C_f = \frac{\epsilon\epsilon_0 A}{D_p} \tag{1}$$

where ϵ_0 represents the vacuum permittivity, A is an effective area, ϵ shows a dielectric constant, and D_p is the thickness of a passive layer which can be qualitatively defined by C_f .

The value of C_f reduces as the Si content increases (table 2), which shows that the thickness of the passive layer increased and the protective capacity improved when the Si content of carbon steel bar gradually increased. Moreover, the value of R_f increased as the Si content in alloyed steel increased, which reveals that the protective property of passive layer was strongly developed. Comparison of C_f and C_{dl} values indicates that C_f was lower than C_{dl} value, confirming the creation of a thin passive layer and also the double-layer in the interfaces had the great capacitive behavior.

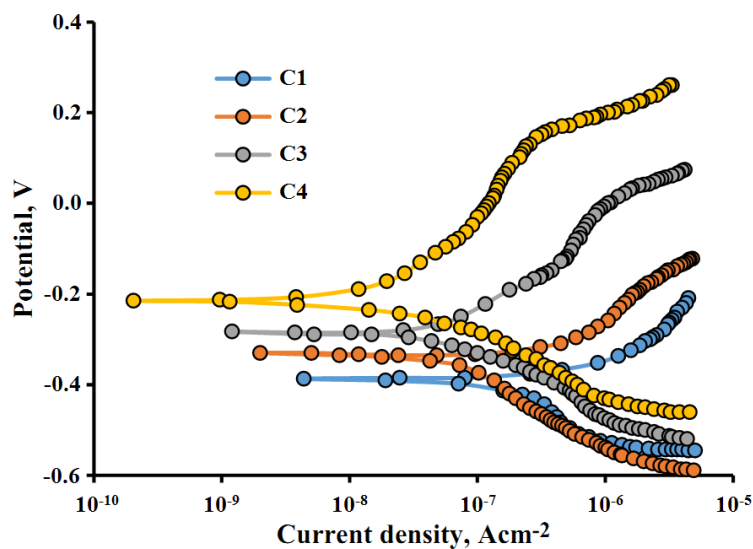


Figure 3. Polarization plots of carbon steel bars with different content of Si in concrete pore solution at pH value of 13 and 1 mV/s scanning rate after one month immersion time.

Potentiodynamic polarization technique is a predictable electrochemical method to consider the corrosion rate of the specimens. From polarization curves in Figure 3, sample C4 reveals most positive in corrosion potential and significant passivation in pore solution.

Consistent with the Tafel extrapolation technique [21], the corrosion parameters of carbon steel bars were obtained by fitting the polarization plots via the Corrview software. Once the applied potential value is sufficiently far from the electrochemical corrosion potential, the polarization plot reveals only kinetics information of an electrode process in the cathodic or anodic branch. Thus, the linear polarization diagram can be extrapolated in an intersection, which offers the values of i_{corr} and E_{corr} [22]. Table 3 indicates the value of electrochemical parameters.

Table 3. Electrochemical parameters of the samples attained from polarization diagrams in concrete pore solution at pH value of 13 and 1 mV/s scanning rate after one month immersion time.

Steels	Corrosion current density (μAcm^{-2})	Corrosion potential (mV)	β_c (mVdec^{-1})	β_a (mVdec^{-1})
C1	0.849	-398	47	85
C2	0.612	-339	54	93
C3	0.109	-286	66	89
C4	0.057	-212	74	85

The level of corrosion can be introduced in four levels suggested by Durar Network Specification [23]. The steel bar with 0.57% Si content had minimum corrosion-current density compared to the other specimens which was in passive state during the experiment.

The E_{corr} of the 0.57% Si specimen was noticeably shifted to higher positive value than the other specimens, which reveals that self-corrosion potential was improved after the addition of Si. Furthermore, the cathodic curves of the samples shifted downwards as the Si concentration increased, which indicated that the cathode reaction rates at this stage was comparatively low. Additionally, cathodic (β_c) and anodic (β_a) Tafel slopes were measured by the Tafel extrapolation method. As revealed in table 3, β_a and β_c values were varying with changing in the Si content. The variations in the value of Tafel slopes can be employed to identify the inhibition process (anodic or cathodic) for carbon steel bars, the charge-transfer coefficient, the electrolyte concentration and the composition of working electrodes [24]. The β_c value considerably unchanged with the addition of Si, which proposes that its cathodic reaction effect did not develop the hydrogen evolution discharge process [25]. However, the anodic Tafel slope values changed significantly with the Si addition which indicates that there are blockages in the anodic reaction sites, and hence affect the anodic reaction mechanism. Furthermore, with increasing Si content, the anode Tafel slopes increased which means that Si element can help corrosion protection of the carbon steel bars in concrete pore solution.

Mass-loss and mass-loss rate of carbon steel bars during the exposure time of one month are indicated in Figure 4. Obviously, Continuous corrosion attack causes increased mass-loss, and the average rate of mass-loss of the C4 sample in each interval was less compared to that of the other

samples. According to Figure 4b, the mass-loss rate of all samples reduced quickly during the initial one week and had a slower decline in the rate of mass-loss during long-term corrosion period. Consistent with the previous studies, the decrease of mass-loss rate in carbon steel bars can be related to the effect of mechanical isolation of the corrosion layer onto direct contact between salt mist and the bar matrix [26, 27]. By comparing these types of bars, the C4 bar exhibited a relatively lower mass-loss rate throughout the test period. The average rate of initial mass-loss in the C4 sample was 0.91 $\text{mgcm}^{-2}\text{day}^{-1}$, which was about 25.4% less than that of C1 sample. Furthermore, the average rate of mass-loss in the C4 sample obtained after the electrochemical corrosion period of one month was 0.44 $\text{mgcm}^{-2}\text{day}^{-1}$, which was about 38.8% less than that of C1 sample. The less mass-loss rate for the C4 sample in the initial corrosion can improve the corrosion resistance of the carbon steel matrix before the creation of a dense rust layer on the sample surface. On the other hand, in a long period of corrosion, because the dense rust layers covered the surface of the sample, the positive separation effect will be more significant to retard the diffusion of the corrosive medium. Thus, the lower mass-loss rate in the C4 sample can be attributed to its rust layer.

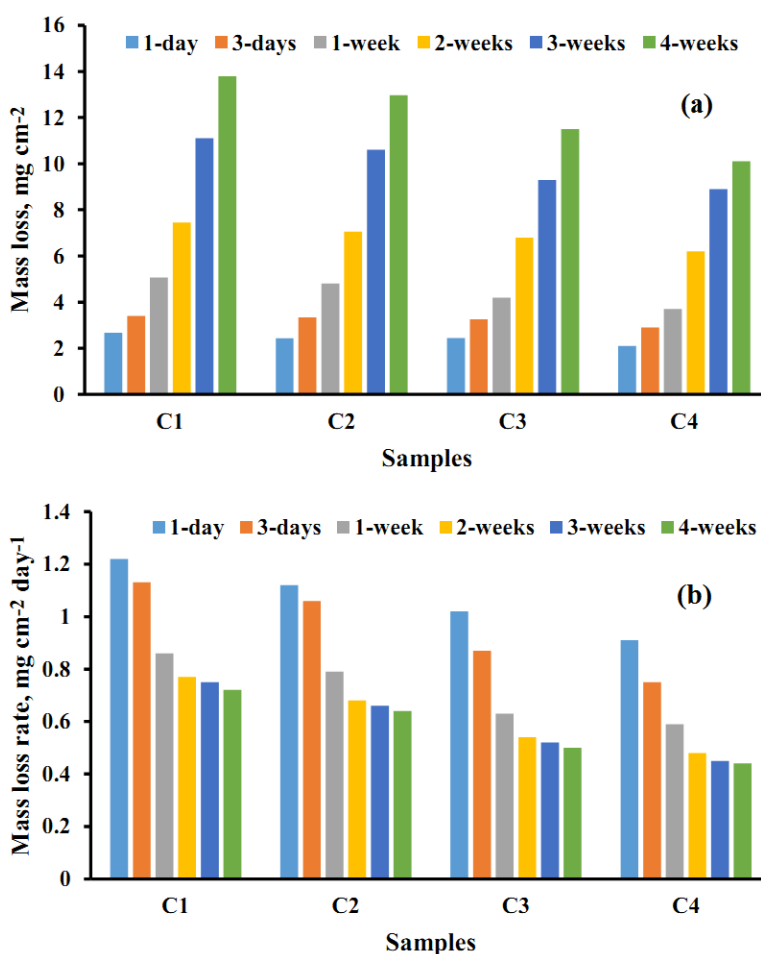


Figure 4. (a) Mass-loss and (b) Mass-loss rate of the carbon steel bars with different Si content during 4 weeks of exposure time in concrete pore solution

Figure 5 shows FESEM images of carbon steel bars in concrete pore solution after one month exposure time. Figure 5b reveals that the carbon steel bar with 0.57 wt% Si was more uniform than the steel bar with 0.42 wt% Si which is in accordance with electrochemical results.

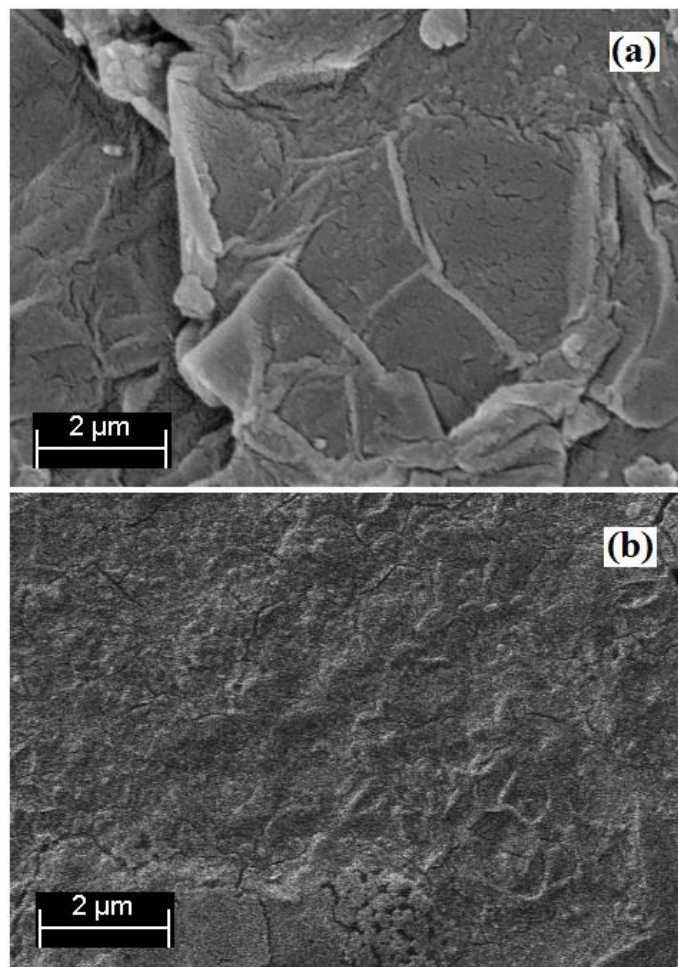


Figure 5. FESEM images of carbon steel bars (a) C1 and (b) C4 samples in concrete pore solution after one month exposure time

4. CONCLUSIONS

Nowadays, alloyed steel rebars have been studied to enhance corrosion resistance of carbon steel rebars in corrosive media which intended to improve the service-life of steel reinforced concrete. In this research, the effects of Si content on the corrosion behavior and passivation of the carbon steel bars in concrete pore solution were studied analytically, and its enhanced corrosion resistance was considered. Electrochemical impedance spectroscopy analysis and polarization techniques were used to investigate the electrochemical corrosion behavior of the samples. The lower mass-loss rate for the steel bar with 0.57 wt% Si content in the initial corrosion indicated an improvement of the corrosion resistance in the carbon steel matrix before the creation of a dense rust layer on the sample surface. The average rate of initial mass-loss in the C4 sample was $0.91 \text{ mgcm}^{-2}\text{day}^{-1}$, which was about 25.4%

less than that of C1 sample. The polarization plots exhibited that the steel bar with 0.57% Si content had minimum corrosion-current density compared to the other specimens which were in passive state during the experiment. The higher value of polarization resistance presents the superior corrosion resistance in C4 samples compared to the other samples. The electrochemical results show that micro-alloying of Si element in the carbon steel bar matrix improved its corrosion resistance against chloride ion attack and delayed the corrosion initiation into the steel matrix. FESEM images of the specimens indicated that the surface of the carbon steel bar with 0.57wt% Si was smooth and no noticeable corrosion was found.

References

1. E. Abbasi, Q. Luo and D. Owens, *Materials Science and Engineering: A*, 725 (2018) 65.
2. S. Jiang, F. Chai, H. Su and C. Yang, *Corrosion Science*, 123 (2017) 217.
3. R.M. Bandeira, J. van Drunen, G. Tremiliosi-Filho, J.R. dos Santos Júnior and J.M.E. de Matos, *Progress in Organic Coatings*, 106 (2017) 50.
4. M.R. Bafandeh, A. Omid and A. Irankhah, *Surface and Coatings Technology*, 315 (2017) 268.
5. S. Kakooei, H.M. Akil, A. Dolati and J. Rouhi, *Construction and Building Materials*, 35 (2012) 564.
6. H. Mohammadhosseini and M.M. Tahir, *Construction and Building Materials*, 180 (2018) 92.
7. J. Rouhi, C.R. Ooi, S. Mahmud and M.R. Mahmood, *Electronic Materials Letters*, 11 (2015) 957.
8. R.R. Hussain, A. Al-Negheimish, A. Alhozaimy and D. Singh, *Cement and Concrete Composites*, 113 (2020) 103728.
9. S. Yadav, S. Gangwar and S. Singh, *Materials Today: Proceedings*, 4 (2017) 5571.
10. M. Alimanesh, J. Rouhi and Z. Hassan, *Ceramics International*, 42 (2016) 5136.
11. Y. Tian, C. Dong, G. Wang, X. Cheng and X. Li, *Construction and Building Materials*, 246 (2020) 118462.
12. J. Fan and Q. Zhang, *International Journal of Electrochemical Science*, 15 (2020) 7624.
13. D. Song, J. Hao, F. Yang, H. Chen, N. Liang, Y. Wu, J. Zhang, H. Ma, E.E. Klu and B. Gao, *Journal of Alloys and Compounds*, 809 (2019) 151787.
14. V. Sharma and A. Shahi, *Journal of Materials Processing Technology*, 253 (2018) 2.
15. X. He, F. Deng, T. Shen, L. Yang, D. Chen, J. Luo, X. Luo, X. Min and F. Wang, *Journal of colloid and interface science*, 539 (2019) 223.
16. R. Mohamed, J. Rouhi, M.F. Malek and A.S. Ismail, *International Journal of Electrochemical Science*, 11 (2016) 2197.
17. F. Husairi, J. Rouhi, K. Eswar, C.R. Ooi, M. Rusop and S. Abdullah, *Sensors and Actuators A: Physical*, 236 (2015) 11.
18. H. Luo, C. Dong, X. Li and K. Xiao, *Electrochimica Acta*, 64 (2012) 211.
19. J. Rouhi, M.R. Mahmood, S. Mahmud and R. Dalvand, *Journal of Solid State Electrochemistry*, 18 (2014) 1695.
20. V. Maurice, H. Peng, L.H. Klein, A. Seyeux, S. Zanna and P. Marcus, *Faraday discussions*, 180 (2015) 151.
21. Y. Xu, C. Zhu, S. Chen, Y. Zhang, T. Wu, X. Lu, M. Wang and X. Feng, *International Journal of Electrochemical Science*, 14 (2019) 9726.
22. S. Zhang, Z. Li, X. Su and C. Yang, *International Journal of Electrochemical Science*, 14 (2019) 10888.

23. R. Galván-Martínez, C. Gaona-Tiburcio and F. Almeraya-Calderón, *International Journal of Electrochemical Science*, 11 (2016) 2994.
24. Y. Zhou, S. Xu, L. Guo, S. Zhang, H. Lu, Y. Gong and F. Gao, *RSC Advances*, 5 (2015) 14804.
25. S. Kakooei, H.M. Akil, M. Jamshidi and J. Rouhi, *Construction and Building Materials*, 27 (2012) 73.
26. H. Tamura, *Corrosion Science*, 50 (2008) 1872.
27. R.E. Melchers, *Corrosion Science*, 68 (2013) 186.

© 2020 The Authors. Published by ESG (www.electrochemsci.org). This article is an open access article distributed under the terms and conditions of the Creative Commons Attribution license (<http://creativecommons.org/licenses/by/4.0/>).